Insights into the loss factors of phytoplankton blooms: The role of cell mortality in the decline of two inshore *Alexandrium* blooms

Chang Jae Choi[1,3], Michael L. Brosnahan[2], Taylor R Sehein[2], Donald M. Anderson[2] and Deana L. Erdner[*,1]

[*]Corresponding author: Deana L. Erdner, The University of Texas at Austin, Marine Science Institute, Port Aransas, TX 78373 USA phone: +1 361 749 6719; fax: +1 361 749 6777; e-mail: derdner@utexas.edu

[1]The University of Texas at Austin, Marine Science Institute, Port Aransas, TX 78373 USA

[2]Biology Department, Woods Hole Oceanographic Institution, Woods Hole, MA 02543 USA

[3]Current address: Monterey Bay Aquarium Research Institute, 7700 Sandholdt Road, Moss Landing, CA 95039 USA

Running head: Cell death in a harmful algal bloom

Keywords: Phytoplankton bloom dynamics; Harmful Algal Blooms (HABs) declines; Phytoplankton mortality; Programmed cell death (PCD); Life cycle transitions; *Alexandrium fundyense*

Abstract

While considerable effort has been devoted to understanding the factors regulating the development of phytoplankton blooms, the mechanisms leading to bloom decline and termination have received less attention. Grazing and sedimentation have been invoked as the main routes for the loss of phytoplankton biomass, and more recently, viral lysis, parasitism and programmed cell death (PCD) have been recognized as additional removal factors. Despite the importance of bloom declines to phytoplankton dynamics, the incidence and significance of various loss factors in regulating phytoplankton populations have not been widely characterized in natural blooms. To understand mechanisms controlling bloom decline, we studied two independent, inshore blooms of *Alexandrium fundyense*, paying special attention to cell mortality as a loss pathway. We observed increases in the number of dead cells with PCD features after the peak of both blooms, demonstrating a role for cell mortality in their terminations. In both blooms, sexual cyst formation appears to have been the dominant process leading to bloom termination, as both blooms were dominated by small-sized gamete cells near their peaks. Cell death and parasitism became more significant as sources of cell loss several days after the onset of bloom decline. Our findings show two distinct phases of bloom decline, characterized by sexual fusion as the initial dominant cell removal processes followed by elimination of remaining cells by cell death and parasitism.

Introduction

Phytoplankton dynamics are driven by imbalances between growth and loss processes that in turn are controlled by a combination of physical (e.g. temperature, light, turbulence), chemical (e.g. nutrients, oxygen) and biological (e.g. life cycle, grazing) factors (Cloern 1996). Blooms occur when growth processes are dominant over losses, then decline when loss processes intensify relative to growth. The mechanisms underlying loss processes are diverse and poorly constrained. Traditionally, grazing by heterotrophic zooplankton and sinking into the deep ocean have been considered the main loss factors for phytoplankton (Calbet and Landry 2004). However, natural populations and laboratory cultures often collapse abruptly due to massive cell lysis events, indicating that different processes must be contributing to phytoplankton mortality (Berges and Falkowski 1998; Vardi et al. 1999; Berges and Choi 2014). Virus-induced cell lysis is increasingly recognized as an important alternative loss factor, with a large number of viruses found in aquatic ecosystems (Brussaard 2004). There is evidence that chronic parasitic infections can be an important cause of phytoplankton population crashes as well (Chambouvet et al. 2008).

Another loss mechanism that has received increased attention in recent years is autocatalyzed cell mortality, such as programmed cell death (PCD). PCD is different from other pathways of cell death because it is an active process that is initiated by the cell itself and tightly controlled by gene expression and protein synthesis inside of the cells (Bidle and Falkowski 2004). Accumulating evidence suggests that PCD occurs in phytoplankton under diverse environmental stresses, such as light and nutrient deprivation, high temperature and salinity, UV exposure and oxidative stress in both

laboratory and natural populations (Segovia et al. 2003; Bidle and Bender 2008; Jauzein and Erdner 2013). Thus, PCD is another potentially important pathway for phytoplankton mortality that can explain abrupt bloom termination in some natural and laboratory systems. Indeed, PCD as an agent for bloom termination has been described in naturally-occurring blooms of the dinoflagellate *Peridinium gatunese* and the haptophyte *Emiliania huxleyi* (Vardi et al. 1999; Vardi et al. 2009). However most attention has been focused on laboratory systems; cell mortality due to PCD and other types of cell death during natural blooms has been much less studied.

Because of their ability to produce potent toxins and therefore cause human poisonings, harmful algal blooms (HABs) have been the subject of intense laboratory and field studies with respect to their ecology, physiology and toxicology (Smayda 1997; Anderson et al. 2005; Erdner et al. 2008). This has resulted in a significant improvement in our understanding of their population dynamics and the underlying processes that lead to the initiation of blooms as well as their subsequent growth and transport pathways. It is generally recognized that populations of benthic life cycle stages or "seedbeds" are key components triggering HAB initiation as they provide the inoculum for blooms (Anderson and Wall 1978; Anderson and Keafer 1985; Garces et al. 2010). These benthic stages can also assist the anthropogenic spread of these organisms, enabling transport under adverse conditions as sometimes occurs in ships' ballast waters or during transplantation of aquaculture animals (Hallegraeff 1993). In some regions, other environmental factors shown to influence bloom formation include enhanced rainfall, freshwater runoff and stabilization of the water column (Therriault et al. 1985; Paerl

1997; Weise et al. 2002). As with phytoplankton in general, the causes of HAB decline are less well understood and constrained.

In this study, the dinoflagellate *Alexandrium fundyense* (previously identified as *A. tamarense* Group I; Lilly et al. 2007; John et al. 2014) was chosen for studying algal bloom dynamics. *A. fundyense* is found in temperate coastal waters worldwide and is a cause of paralytic shellfish poisoning (PSP). For this reason, the physiology, ecology and toxicity of this organism has been investigated extensively in both laboratory and field contexts, making it one of the most well-studied marine unicellular algal species. Past studies have linked the progression of *A. fundyense* blooms to life cycle transitions, from vegetative reproduction during bloom development to sexual fusion and encystment where gametes are formed and fuse to produce a planozygote and later a benthic resting cyst (e.g., Anderson 1998). Quantification of planozygotes during blooms suggests that a significant fraction of the bloom population forms cysts, emphasizing the importance of sexual fusion to bloom termination (Anderson et al. 1983; McGillicuddy et al. 2014; Brosnahan et al. 2015). Other possible contributors to bloom decline include grazing (Petitpas et al. 2015) and parasitism by *Amoebophrya* spp. dinoflagellates (Velo-Suarez et al. 2013). *Amoebophrya* spp. infect *A. fundyense* as free-swimming dinospore cells (~3 μm in diameter), then invade the cytosol and nucleus of their host, undergoing multiple rounds of nuclear division and flagellar replication as they form a trophont within the *A. fundyense* cell. Maturation of the trophont eventually leads to lysis of the host cell, releasing tens to hundreds of new infective dinospores (Cachon 1964). Similar attack of *A. fundyense* by viruses has not been described, and therefore the role of virus-mediated cell death is unknown. Like many other HABs, the timing and mechanisms involved in

the end of *A. fundyense* blooms have considerable socio-economic and ecological implications (Erdner et al. 2008; Anderson 2009). Some HAB species can constitute a large fraction of the phytoplankton biomass during blooms, so cell loss can affect not only community structure and function, but also food web dynamics, toxin dynamics and element cycling.

The primary objective of this study was therefore to explore the extent to which cell death processes contribute to *A. fundyense* bloom termination. In particular, we quantified temporal and spatial (depth) changes in natural populations of *A. fundyense* including markers of cell mortality over the course of two inshore blooms. We addressed the role of cell death, in particular PCD, as a contributor to bloom demise and compared its impact as a loss process to infections by *Amoebophrya* parasites. We also placed cell death observations in the context of life cycle transitions by the *A. fundyense* population and evaluated the relative contribution of various loss processes to bloom decline.

Materials and methods

Study sites

The NMS (Nauset Marsh System; Eastham, MA USA) is a network of drowned, tidal kettle ponds connected to each other through shallow, marsh channels and to the Atlantic Ocean via Nauset Inlet (Fig. 1). Salt Pond and Mill Pond are the northern and southern extremities of this system and are significantly deeper than the shallow central marsh area (1.25 m average depth, compared to 9 m and 11 m maximum depths in Salt Pond and Mill Pond, respectively; Crespo et al. 2011). Both ponds experience semidiurnal tides that range from 1-2 meters through the neap-spring cycle. Selective retention of *A.*

fundyense populations and a north-south temperature gradient across the NMS cause blooms in the two ponds to experience independent development and termination that are staggered in time by 2-3 weeks (Crespo et al. 2011; Ralston et al. 2014). This characteristic of the NMS enabled us to investigate two independent *A. fundyense* blooms through their complete bloom cycle, from development through their peak and termination phases within a single field campaign.

A. fundyense bloom monitoring

Phytoplankton samples were taken weekly at stations over the deepest areas of Mill Pond (~11 m deep) and Salt Pond (~9 m deep), from early March to late May 2013. Samples were collected during daylight hours and, to the extent possible, near high tide. Actual timing varied due to the logistics associated with accessing the two study locations by land on a single day. Sample times in Mill Pond varied from 10:30 h to 12:00 h and from 11:30 h to 14:30 h in Salt Pond. Tidal cycles at these two locations are highly correlated in time and are characterized by rapid floods (~4 h) and slow ebbs (~8 h). Sampling at Salt Pond was always conducted near high water and usually during ebbs so that additional samples could be collected from shallow areas immediately outside Salt Pond for another study. Sampling at Mill Pond was always completed before sampling at Salt Pond and about a third of these latter samples were collected during floods.

In Salt Pond, sampling included triplicate 5 L Niskin samples from 1 and 5 m depths and single Niskin samples from depths of 3 m and 1 m above the bottom, over a deep hole, roughly in the center of Salt Pond. In Mill Pond, single 5 L Niskin samples were collected from 1, 3, 5 and 7 m depths as well as 1 m from the bottom, over a deep hole

near the northern shore of the pond. *Alexandrium* counts were made from 2 L subsamples of each Niskin collection. These subsamples were concentrated over 20 µm Nitex mesh and fixed with 5% unbuffered formalin in the field before being placed on ice for transport back to the laboratory where they were then resuspended in ice-cold methanol and stored at -20˚C until final preparation for counting. Additional 200 mL subsamples were collected from one Niskin bottle at each depth sampled in Salt Pond only for abundance estimation of *Amoebophrya* spp. dinospores. These smaller subsamples were fixed in the field with 2.5% formalin (v/v) and stored on ice for transport to the laboratory where dinospores were concentrated on 0.8 µm polycarbonate filters and serially washed with 50%, 80% and 100% ethanol solutions prior to storage in a -20˚C freezer until preparation for counting.

Samples for estimation of *A. funydense* abundance were prepared for counting by staining with a species-specific oligonucleotide probe (NA1; 5'-AGT GCA ACA CTC CCA CCA-3') as previously described by Anderson et al. (2005). *Amoebophrya* dinospore abundance was assessed using fluorescence in situ hybridization with tyramide signal amplification (FISH-TSA) as described by Velo-Suarez et al. (2013).

The same FISH-TSA protocol was modified as follows to assess infection prevalence in *A. fundyense* host cells that had been fixed and stored as described for abundance estimation using the NA1 oligonucleotide probe. Subsamples of the methanol suspensions containing ~100 cells were concentrated on 0.8 µm polycarbonate filters mounted on a vacuum manifold and without agarose embedding. Samples were left mounted on the manifold, which was used to remove block and stain solutions with minimal manipulation of filters (preventing *A. fundyense* cell loss). This change required

the staining solution to be made without addition of dextran sulfate and blocking agent in order to reduce filter clogging. After TSA development, filters were carefully removed from the manifold, mounted on individual slides and stored at 4˚C until examination by epifluorescence microscopy. Whole filters were scanned for *A. fundyense* host cells and individual infections were graded 'early' if detectable as a small dot within the host cell, 'intermediate' if an *Amoebophrya* cell cluster was present and 'mature' if the parasite had formed a multinuclear trophont.

Sampling for PCD markers

Water samples for assessment of PCD markers were collected alongside (and in addition to) samples for *A. fundyense* monitoring with additional samples collected on 9 May and 17 May in Salt Pond to better characterize that bloom's termination phase. Whole seawater samples of 4 L were collected using single 5 L Niskin bottles from four discrete depths in Salt Pond: the near-surface (0-1 m), mid-depth (approximately 3 and 5 m) and near-bottom (approximately 7 m), while two depths (5 m and 7 m depths) were chosen for Mill Pond where the maximum concentration of *A. fundyense* cells were typically observed. Samples were immediately stored on ice and brought back to the laboratory for sample processing and analysis. In the laboratory, samples were prescreened with 125 μm and 80 μm pore size sieves to sequentially remove large plankton and detritus, and concentrated by retention of cells on 20 μm Nitex mesh. Cells were then backwashed with filtered seawater to a final volume of 30 mL and triplicate 1 mL aliquots were prepared for observation of viability, PCD, ROS markers and for cell size assessments. Three, 1 mL aliquots were also taken from each PCD marker sample, preserved with

Lugol's iodine solution (1% final concentration), and counted using a 1mL Sedgewick-Rafter counting chamber to provide additional *A. fundyense* cell abundance estimates alongside cell counts from separate Niskin samples used for the bloom monitoring.

A. fundyense viability assay

Cell viability was evaluated using both Evans Blue (final concentration of 1:2000 (w/v) of 1% stock (w/v)) (Crippen and Perrier 1974) and Zombie Aqua (BioLegend, San Diego, CA USA) according to the manufacturers' instructions. Cells with intact plasma membranes exclude the Evans Blue dye, whereas the dye penetrates and stains dead cells. Zombie Aqua reacts with primary amine groups on proteins, and dead cells show increased protein labeling as the dye penetrates into the cytoplasm while live cells are only labeled with surface proteins. An advantage of the Zombie Aqua dye is that live-dead determinations can be made after fixation, enabling postponement of analysis for some time after treatment. In contrast, cells treated with Evans Blue need to be analyzed within a few hours to ensure accurate viability estimates. In both assays, cell viability was assessed from three 1 mL subsamples using a Zeiss Axioskop epifluorescence microscope outfitted with a DAPI/Hoeschst filter set (excitation wavelength 365/50 nm and emission of 445/50 nm).

In situ detection of PCD markers

A distinctive feature of PCD is the activation of caspase enzymes. Caspase activity was assayed with Image-iT™ LIVE Green Poly Caspases Detection Kit (Invitrogen, Carlsbad, CA USA), which is based on a fluorescent inhibitor of caspases (FLICA™).

Cells were harvested by centrifugation at 1000 × g for 5 min, resuspended in 1X FLICA working reagent, and incubated for 60 min at room temperature in darkness. Cells were washed twice with wash buffer and fixed before analyzing under a Zeiss Axioskop epifluorescence microscope outfitted with a FITC filter set (excitation wavelength 470/40 nm and emission of 525/50 nm). Measurements from each sample were made from three 1 mL aliquots.

ROS detection assay

Levels of intracellular reactive oxygen species (ROS), known mediators for PCD, were measured using the oxidation-sensitive fluorescent probe, carboxy-H_2DCFDA [5-(and 6)-carboxy-2',7'-dichlorodihydrofluorescein diacetate] (Invitrogen, Carlsbad, CA USA). Aliquots (1 mL) of samples were centrifuged at 1000 × g for 5 min. The supernatant was carefully discarded, and the pellet was resuspended in 1 mL of 10 mM PBS buffer, pH 7.5 containing a final concentration of 5 μM H_2DCFDA and incubated for 60 min at 20˚C in darkness. Cells were then washed twice with PBS. Green DCF fluorescence of cells was observed with a Zeiss Axioskop epifluorescence microscope equipped with a FITC filter set (excitation wavelength 470/40 nm and emission of 525/50 nm).

Measurement of *A. fundyense* cell size distributions

A. fundyense cells fixed with 5% unbuffered formalin were captured from random fields of view, and the number of cells and their areas were estimated using ImageJ software (National Institute of Health, Bethesda, MD USA) following a protocol for single cell area measurements outlined by Papadopulos et al. (2007). Briefly, measurements from

cell images collected under 200x magnification were calibrated according to a 20 μm standard under the same magnification. Cell sizes were determined automatically using the "Analyze Particles" function in ImageJ, which applied an automated threshold for detection of cell boundaries and calculated minimum, maximum and equivalent spherical diameters. In turn, individual cell volumes were estimated using a spherical approximation. Cell size was used as an indicator of life cycle stage following criteria applied by Brosnahan et al. (2015). Late-stage planozygotes were defined as large cells greater than 43 μm in an equivalent circular diameter based on previous descriptions (Anderson et al. 1983), and gametes were defined as cells smaller than 30 μm in an equivalent circular diameter (Brosnahan et al. 2015). This corresponds to the smallest 5% of cell volumes observed in samples from the start of the *A. fundyense* bloom in Salt Pond (sample collected 22 April). Partitioning of the population into gamete, vegetative cell and late-stage planozygotes was then assessed by determining the proportion with volumes <14,137 μm^3, >14,137 μm^3 and <41,630 μm^3, and >41,630 μm^3, respectively.

Results

A. fundyense population dynamics in Mill Pond and Salt Pond

Our results from the overall water column analysis revealed that *A. fundyense* was the dominant phytoplankton species and the maximum cell concentrations were mostly observed in subsurface samples - either from 3 or 5 m depth in Salt Pond and 5 or 7 m depth in Mill Pond - and surface cell concentrations remained low throughout the bloom period (Fig. 2). We used depth samples where the maximum cell numbers were observed as the most representative sample for the *A. fundyense* population in both ponds. At the

beginning of the sampling period (25 March), the bloom had already started in Mill Pond as *A. fundyense* mean concentration was greater than ~6,000 cells L^{-1} at 7 m depth (data not shown). *A. fundyense* concentrations continued to increase until the bloom peaked on 29 April with maximum concentrations of ~2.2×10^6 cells L^{-1}, about a month after the first sampling period. Subsequently, cell abundance decreased about 6-fold (~3.5×10^5 cells L^{-1}) over the next week and dramatically declined >350-fold the following week to ~1,000 cells L^{-1} (Fig. 2a).

The peak of the bloom in Salt Pond was nearly two weeks later than the Mill Pond peak (9 May vs. 29 April in Mill Pond), however development of the bloom was much faster than Mill Pond (1 Apr - 29 Apr in Mill Pond vs. 22 Apr - 9 May in Salt Pond). Concentrations of *A. fundyense* in Salt Pond peaked on 9 May, reaching ~1×10^6 cells L^{-1}. *A. fundyense* concentrations decreased dramatically over the next week (9-17 May), declining 66-fold (to ~15,000 cells L^{-1}) on 17 May and remaining less than 1,000 cells L^{-1} through the end of the sampling period.

Cell death, PCD and infections in *A. fundyense*

Less than 5% dead cells were detected during the development phase including the peak of the blooms in both Mill and Salt Ponds. However, in Mill Pond over 10% dead cells were observed during termination (6 May, 14.1% at 7 m depth). Fewer dead cells were observed a week later, though overall *A. fundyense* abundance was down as well (13 May, 8.3% at 5 m depth, ~1,000 cells L^{-1}; Fig. 3a). A similar but less intense pattern of cell mortality was observed in Salt Pond where very few dead cells were detected up to the peak of the bloom. Dead cells then increased as a proportion of the population during

termination (6.8% on 13 May and 5.5% on 17 May at 5 m depth; Fig. 3b). Caspase activity was measured only in Salt Pond, where active caspase levels increased in parallel with dead cells after the bloom's peak (Fig. 3b).

Another common feature of PCD is intracellular ROS production, which serves as a trigger for cell death. Cells exhibiting endogenous ROS generation were observed about two weeks prior to the bloom peak both in Mill Pond and Salt Pond, but were barely detected otherwise (Fig. 3a and 3b). An exception was the end of the bloom in Salt Pond, where cells showed a dramatic increase in ROS generation (35.5 ± 3.0% on 17 May at 5 m depth) on our last sampling date (Fig. 3b).

In Salt Pond, *Amoebophrya* dinospores were observed throughout the bloom period and their abundance remained relatively constant until the bloom's termination when dinospore abundance increased sharply. This spike in dinospore abundance was preceded by a similar increase in the prevalence of *Amoebophrya* infections near the bloom's peak. Prevalence estimates from earlier in the bloom's development were less than 5% for all infection stages, but increased to a combined 26.7% after the bloom's peak (Fig. 3c). The impact of parasitic infections and cell death was further examined over depth (Fig. 3d). Prior to the bloom peak, higher infection rates were observed at 3 m than at 5 m on 29 Apr and 6 May (5.8% and 13.1% at 3 m and 3.3% and 7.1% at 5 m depth, respectively). Similarly, increased numbers of dead cells were found at 3 m than at 5 m depth although the prevalence of infections was higher than the proportions of dead cells. A distinct depth distribution was observed during bloom decline (13 May) when infections were more prevalent at 5 m (26.7%) than at 1 m (13.5%), but dead cells were proportionally

more abundant closer to the surface (26.8% at 1 m compared to 5.0% at 3 m and 6.8% at 5 m; Fig. 3d).

Cell size distributions over the course of the *A. fundyense* bloom in Salt Pond

A. fundyense cell sizes were measured and compared over the bloom period to track cells potentially representing three distinct life-cycle stages - vegetative cells, gametes and planozygotes - based on their size. Though vegetative cell size varies over the light:dark cycle in natural populations (e.g. Brosnahan et al. 2015), sexual life cycle transitions are clearly recognizable from large shifts in bloom populations toward smaller (gamete) and larger (mature planozygote) cells (Fig. 4a and Supplementary Fig. S1). During the early phase of the bloom in Salt Pond, the *A. fundyense* population was dominated by vegetative cells (96.4%), volumes between 14,172 μm^3 and 36,998 μm^3 (mean: 22,848.7 μm^3, 22 Apr; Supplementary Table S1 and Fig. 4b). Small and large cells, gametes and late-stage planozygotes respectively, were also detected at this time, but were each less than 4% of the total population and therefore were more likely especially large and small mitotic stages (3.2% gametes, cells smaller than 14,137 μm^3 and 0.4% planozygotes, cells larger than 41,630 μm^3). As the bloom continued to develop, the population remained dominated by vegetative cells with 84% of cells still within the vegetative cell size range (29 Apr). Mean cell size continued to decrease until the peak of the bloom where most cell sizes were less than 20,000 μm^3 with a mean size of 12744.1 μm^3 on 9 May - roughly half of the mean cell volume measured on 22 April (Supplementary Table S1). Very small cells (less than 10,000 μm^3) were over 47% of the population at this time (Supplementary Figure S1). The mean cell size in the population then increased abruptly,

with a mean size of 27091.9 μm^3 as the bloom declined (13 May). The mean cell size continued to increase up to 32987.4 μm^3 at the end of the bloom (Supplementary Table S1 and Fig. 4a). While most of these post bloom peak cells were classified as vegetative cells by our size criteria, they are more likely to have been early stage planozygotes, which can be comparable in size to vegetative cells (Brosnahan et al. 2014; Brosnahan et al. 2015).

Discussion

Evidence of cell death during *A. fundyense* bloom decline

Over the past decade, concepts of phytoplankton cell death have evolved rapidly with the discovery that phytoplankton often die spontaneously through processes independent from grazing and sedimentation (Franklin et al. 2006; Berges and Choi 2014). Cell mortality caused by PCD has received more attention since accumulating physiological and biochemical data collectively suggest that PCD is triggered by diverse environmental cues, often when phytoplankton encounter adverse environmental conditions (Bidle and Falkowski 2004). The presence of an operational PCD molecular machinery, e.g. metacaspases in phytoplankton genomes, indicates PCD was established early in the evolution of unicellular phytoplankton and therefore is potentially important for phytoplankton bloom dynamics (Choi and Berges 2013). However, the role of PCD has not been widely examined in natural populations. The one other study of which we are aware focused on an *E. huxleyi* bloom where PCD was associated with the spread of viral infections (Vardi et al. 2012). Our study uniquely has assessed the occurrence of PCD and other cell death through the full course of an algal species' bloom cycle, from its

development through its demise and contrasts the impact of cell death on bloom demise to that of other loss pathways, particularly infections by an intracellular parasite (*Amoebophrya* spp.) that chronically impacts inshore dinoflagellate blooms.

Cell mortality was quantified in an effort to understand the role of cell death in bloom dynamics, particularly its contribution to the termination of blooms of the toxic dinoflagellate *A. fundyense*. Dead cells were barely detected during the early phase of development through bloom peaks, indicating that most cells were actively growing. Increases in cell mortality were observed only after *A. fundyense* cell abundance had already declined sharply. The highest proportions of dead cells measured in the Mill Pond and Salt Pond populations were between 5 and 15% (Fig. 3a and 3b). These results indicate that cell death was a significant cell loss pathway during the late stages of both *A. fundyense* blooms recorded. In particular, we observed *A. fundyense* cells exhibiting features of PCD (intracellular ROS generation and caspase activity) during bloom decline, suggesting the presence of PCD as a cell death pathway in *A. fundyense*. Genes encoding metacaspases, molecular executioners that initiate PCD processes, are found in *Alexandrium* species (Choi et al. manuscript in prep), and increased metacaspase activity was observed under stressful conditions suggesting the presence of PCD in *A. fundyense* (Jauzein and Erdner 2013).

Interestingly, a drastic increase in ROS level was detected at the end of the bloom period in Salt Pond (Fig. 3a and 3b), indicating that *A. fundyense* cells were stressed. In other systems ROS generation has been associated with active host defense against parasite infection (Lu et al. 2014). The *A. fundyense* in Salt Pond were also observed to suffer from *Amoebophrya* infections at the end of the bloom, with infection prevalence

comparable to observations made during the previous year's bloom (Velo-Suarez et al. 2013). However, in Mill Pond where infections were also observed, though with lower prevalence, a similar ROS spike was not observed. The Mill Pond population may have had a lesser parasite challenge than the Salt Pond population or a parasite-associated ROS spike in Mill Pond was simply missed by our sampling. Increased ROS generation was also observed in both Mill and Salt Ponds during bloom development - about two weeks before each bloom's peak - without noticeable cell death and only minimal levels of parasitism. It is not clear what triggered these earlier elevated ROS levels, since no spikes in dinospore abundance or cell infections were observed at those times (Fig. 3c). ROS production has also been shown to increase during bloom development in *Peridinium* due to CO_2 limitation (Vardi et al. 1999), underscoring its generalized association with stress on algal cells. Our results suggest that *A. fundyense* may experience transient stressful conditions during rapid growth, but such conditions, at least in the case of these blooms, did not slow bloom development to an appreciable extent.

Other sources of cell loss

Cell death is just one of many loss processes that contribute to *A. fundyense* bloom termination. For phytoplankton generally, grazing, viral lysis and parasite infection are recognized sources of mortality. In the case of *A. fundyense*, life cycle transitions have been shown to play a major role in the termination of both inshore and offshore blooms, specifically the shift from vegetative reproduction during the early phase of blooms to sexual encystment, a process which begins when gametes are formed and ends when new

zygotic resting cysts are recruited to the ocean bottom (Anderson et al. 1983; McGillicuddy et al. 2014; Brosnahan et al. 2015).

It has been difficult to quantify the different life cycle stages, since vegetative cells, gametes and planozygotes are morphologically similar to one another, but work by Brosnahan et al. (2015) directly linked the production of small cells with gametogenesis in Salt Pond. In this study, cell size data is used to estimate the impact of life cycle transitions on the 2013 bloom in Salt Pond (Fig. 4, Supplementary Table S1 and Supplementary Fig. S1). The gamete size range was defined as the smallest 5% of cells (<30 μm equivalent circular diameter, <14,137 μm^3 in volume) present at the start of the bloom, when the population was composed almost exclusively of vegetative cells. Late-stage planozygotes were also identified based on their size, i.e. as cells whose equivalent circular diameter was greater than 43 μm (estimated volume was >41,630 μm^3). Both of these size-based definitions agree well with those established by Brosnahan et al. (2015) from analysis of *A. fundyense* images recorded by an Imaging FlowCytobot. An important limitation of this size-based approach is that it misclassifies early-stage planozygotes as vegetative cells. It's very likely that most vegetative size-class cells present after the bloom's peak were in fact early-stage planozygotes (Brosnahan et al. 2015).

Based on the cell size changes recorded, the proportion of vegetative cells, gametes and late-stage planozygotes was estimated for each sampling day over the full course of the bloom in Salt Pond (Fig. 4b). During the bloom's development, our size criteria classified over 96% of *A. fundyense* as vegetative cells, consistent with prior work that has shown bloom formation in this system to be driven by division rather than cyst

germination (Crespo et al. 2011). While maximum and minimum cell sizes indicated that both gametes and planozygotes were also present during bloom development, this is more likely classification error associated with ongoing mitotic cell division. As the bloom matured, the proportion of vegetative cells decreased markedly, comprising less than 40% of the population at the bloom peak on 9 May (36.1%; Fig. 4b). During the bloom's subsequent decline, the proportion of gametes then dropped drastically, suggesting a significant loss of cells through mating (Fig. 4b).

In contrast to encystment, grazing - though a major loss pathway for other phytoplankton species - appears to have minimal impacts on *A. fundyense* within the Nauset Marsh System. While the grazer community consuming *A. fundyense* is diverse and includes several meso- and microplankton (ciliates, rotifers, heterotrophic dinoflagellates, copepod stages and marine cladocerans; Turner and Anderson 1983; Petitpas et al. 2015) and filter-feeding animals (clams, mussels and oysters), combined loss rates to these grazer populations have been challenging to quantify. Recent work in Salt Pond by Petitpas et al. (2015) showed that grazing did not appear to hinder net growth by *A. fundyense* during bloom development. Similarly, continuous in situ imaging flow cytometry applied by Brosnahan et al. (2015) showed that accumulation of *A. fundyense* was comparable to an estimator of the population's in situ division rate, supporting the contention that grazing only minimally impacts the *A. fundyense* population in Salt Pond.

Inshore populations of *A. fundyense* are also known to be chronically impacted by *Amoebophrya* spp. parasites. In this study, the proportion of infected cells remained low through the peak of both blooms but increased afterwards, up to a maximum of 26.7%

combined for all stages of infection in Salt Pond (Fig. 3c). The temporal pattern and intensity of parasite impact on the bloom was highly similar to the 2012 Salt Pond bloom which had maximum infection prevalence of about 30% during its termination (Velo-Suàrez et al. 2013). Across all samples collected, maximum infection rates were higher than the observed proportion of dead cells, and the proportions of dead cells and infected cells showed contrasting patterns with depth (Fig. 3d). Given these differences in their distribution, we disregard the possibility that some cell death positive cells were also infected by the parasite and instead consider parasite infection and mortality as distinct cell loss pathways.

Relative contribution of loss processes to bloom declines

Our results indicate that parasite infection, cell death and gametogenesis are all pathways for cell loss during the observed *Alexandrium* blooms. Cell numbers in Salt Pond declined precipitously after the bloom peak, with a reduction of 87% between 9 and 13 May, and then 88% of the remainder by 17 May (98% of 9 May population). How much of these losses are attributable to cell death, parasitism, life cycle transitions and other processes such as grazing?

Loss rates from cell death can be estimated from the proportion of cells in a particular state divided by that state's persistence time. In the case of cells infected by *Amoebophyra* spp., the persistence time depends on their stage of infection (Velo-Suarez et al. 2013). For dead cells, persistence can be estimated from cell settling times. While settling time has not been measured directly from dead *A. fundyense* cells, measured settling rates of other comparably sized dinoflagellates are 2-3 m d^{-1} (Kamykowski et al.

1992). Given mean depths across the two NMS ponds, this translates to persistence times of less than half a day. In a sample where 7% of the cells are dead, we estimate that cell death is causing population declines of at least 14% day^{-1}.

For losses to sexual fusion and encystment, the persistence time might correspond to how long a gamete might take to fuse with a second gamete to form a planozygote and then encyst. However, mounting evidence suggests that some planozygotes may divide to regenerate gamete sized cells, complicating a similar, simple adaptation of the persistence time model for estimating encystment losses (Brosnahan et al. 2015; Figueroa et al. 2015) Still, the concerted nature of the bloom's sexual transition is useful for considering what fraction each loss process might contribute to the total decline of the Salt Pond bloom. Through its rapid transition to sexual stages, the bloom essentially stops division, enabling us to ignore population growth after the bloom's peak (Brosnahan et al. 2015). Loss rates from various processes are therefore directly translatable to the total contribution each makes to the blooms' ultimate demise.

We used a simple model to calculate the daily and total loss of cells due to parasitism and cell death during bloom decline. We have observations from 9, 13 and 17 May, and we extrapolated the cell numbers in between by applying an exponential loss curve. The proportion of infected cells was interpolated linearly between observations, and we used the same approach for the estimation of cell mortality. For example, the 2.1% dead cells on 9 May was interpolated linearly to the 28.6% dead cells measured on 13 May and similarly for the interval from 13 May to 17 May. From these approximations, we calculated daily loss contributions from each process to the bloom's overall decline. These calculations are provided in Supplementary Table S2.

Between 9 and 13 May, *A. fundyense* concentrations decreased by about an order of magnitude, daily loss due to infection ranged from 8.8 to 23.4% day^{-1} with a cumulative contribution of 12.7% of the peak bloom population. Daily loss rates due to cell death ranged from 9.9 to 52.9% day^{-1}, and cumulative loss rate was 21.4%. The remaining 65.9% of peak population loss is attributed primarily to encystment but other factors (e.g., grazing and dispersal) also likely contributed. Later during the Salt Pond bloom's decline, between 13 and 17 May, cell numbers were greatly reduced but still high (10^4-10^5 L^{-1}) and cell death and parasitism played a more significant role in the overall loss rate with maximum daily losses of 37.8% to parasitism and 61.6% to cell death.

Combined, cell death and *Amoebophrya* infection account for 42.5% of the bloom's total decline. An important caveat to this estimate is that the calculations are highly sensitive to our underlying assumptions, especially regarding interpolation of cell death and infection rates between sparse data. While these processes certainly have the potential to play major roles in the demise of *A. fundyense* blooms, the high estimate of parasite-induced loss contradicts a recent, intensive study of this same system through which higher maximum infection rates were observed but the total fraction of the population succumbing to infection was estimated to be much lower (Velo-Suarez et al. 2013). Similar intensive studies of cell death that better sample the spatial and temporal patchiness of this process may significantly alter our understanding of the role played by cell death on the demise of *A. fundyense* and other harmful algal blooms.

In all, mating and cyst formation appears to be the dominant process for bloom decline in the Salt Pond system, both in this study (2013) and in 2012 (Brosnahan et al. 2015). This is based upon the rapid synchronous appearance of gametes right before the bloom

peak, coupled with their rapid disappearance immediately afterwards. However, while the gametes undoubtedly disappear from the water column, their ultimate fate is unclear. Planozygote proportions do not increase concurrently or in proportion to gamete disappearance (Fig. 4b; Brosnahan et al. 2015). This could result from rapid encystment, i.e. a short residence time in the pond water column as planozygotes, but post-bloom estimates of cyst abundance within the pond only account for about 10% of the bloom's peak (M.L. Brosnahan unpubl. data). Shoaling of vertical swimming ambits was also observed during the 2013 bloom's sexual transition, suggesting that export from the pond is likely heightened during the bloom's sexual phase. Post-bloom numbers of cysts within the pond therefore likely grossly underestimate the true conversion of the population to sexual stages and retention within Salt Pond may differ between different *A. fundyense* sexual stages (Brosnahan et al. manuscript in prep). More detailed descriptions of export of sexual stage cells is likely to further alter the estimated impacts of cell death and other processes on bloom decline since the calculation described here ignores the possibility that dead cells might be exported from the pond at higher rates than e.g. infected cells, which tended to be distributed deeper in the pond.

Impacts from loss processes besides encystment - parasitism, grazing and cell death - appear to become the main cell loss pathways after the bloom's peak, and therefore after the bulk of the population likely underwent encystment. Adverse conditions trigger encystment of *Alexandrium* in the lab (Anderson et al. 1984), and stressors can induce temporary cysts in clonal culture (Jauzein and Erdner 2013). Thus, *Alexandrium* may be able to avoid adverse conditions by encysting, with other loss processes operating primarily on those cells that are unable to find a mating partner or are slow to mature as

planozygotes. It is also likely that the relative contribution of different loss factors varies depending on the environment. Salt Pond is a relatively contained system where blooms reach very high densities, which should enhance the probability of both gamete encounters and propagation of parasitic infections. In larger, more open systems where blooms typically achieve lower peak cell concentrations, the probability of encountering a compatible gamete may be reduced, increasing the likelihood of cell death or other fates.

Conclusions

Our results indicate that *A. fundyense* cells undergo endogenous cell death, potentially via PCD pathways, during bloom decline. This adds natural cell death as an additional source of cell loss during *A. fundyense* blooms. In the relatively small and contained Salt Pond system, life cycle transitions (i.e., cyst formation) appear to be the biggest contributor to bloom decline, followed by cell death, parasitism and other processes such as grazing. Unlike other phytoplankton that undergo cell death when exposed to adverse conditions, some dinoflagellates including *A. fundyense* can overcome adverse conditions via encystment, so cell death and parasitism may represent the ultimate fates only for those cells that do not manage to successfully complete this life cycle transition. Understanding bloom decline is a high priority with implications for HAB control and prevention, and our results not only contribute significantly to our knowledge of phytoplankton bloom dynamics, but provide a framework for studying other blooms.

References

Anderson, D., S. Chisholm, and C. Watras. 1983. Importance of life cycle events in the population dynamics of *Gonyaulax tamarensis*. Mar. Biol. **76:** 179-189. doi:10.1007/BF00392734

Anderson, D., D. Townsend, D. McGillicuddy, and J. Turner. 2005. The ecology and oceanography of toxic *Alexandrium fundyense* blooms in the Gulf of Maine. Deep Sea Res., Part II **52:** 2365-2368. doi:10.1016/j.dsr2.2005.08.001

Anderson, D. M. 1998. Physiology and bloom dynamics of toxic *Alexandrium* species, with emphasis on life cycle transitions. Nato ASI Ser., Ser. G **41:** 29-48.

Anderson, D. M. 2009. Approaches to monitoring, control and management of harmful algal blooms (HABs). Ocean Coast. Manage. **52:** 342-347. doi:10.1016/j.ocecoaman.2009.04.006

Anderson, D. M., and B. A. Keafer. 1985. Dinoflagellate cyst dynamics in coastal and estuarine waters, p. 219-224. Anderson DM, White AM, and Baden DG [eds.], Toxic Dinoflagellates. New York: Elsevier.

Anderson, D. M., D. M. Kulis, and B. J. Binder. 1984. Sexuality and cyst formation in the dinoflagellate *Gonyaulax tamarensis*: cyst yield in batch cultures. J. Phycol. **20:** 418-425. doi:10.1111/j.0022-3646.1984.00418.x

Anderson, D. M., and D. Wall. 1978. Potential importance of benthic cysts of *Gonyaulax tamarensis* and *G. excavata* in initiating toxic dinoflagellate blooms. J. Phycol. **14:** 224-234. doi:10.1111/j.1529-8817.1978.tb02452.x

Berges, J. A., and C. J. Choi. 2014. Cell death in algae: physiological processes and relationships with stress. Perspect. Phycol. **1:** 103-112. doi:10.1127/pip/2014/0013

Berges, J. A., and P. G. Falkowski. 1998. Physiological stress and cell death in marine phytoplankton: induction of proteases in response to nitrogen or light limitation. Limnol. Oceanogr. **43:** 129-135. doi:10.4319/lo.1998.43.1.0129

Bidle, K. D., and S. J. Bender. 2008. Iron starvation and culture age activate metacaspases and programmed cell death in the marine diatom *Thalassiosira pseudonana*. Eukaryotic Cell **7:** 223-236. doi:10.1128/ec.00296-07

Bidle, K. D., and P. G. Falkowski. 2004. Cell death in planktonic, photosynthetic microorganisms. Nat. Rev. Microbiol. **2:** 643-655. doi:10.1038/nrmicro956

Brosnahan, M. L., S. Farzan, B. A. Keafer, H. M. Sosik, R. J. Olson, and D. M. Anderson. 2014. Complexities of bloom dynamics in the toxic dinoflagellate *Alexandrium fundyense* revealed through DNA measurements by imaging flow cytometry coupled with species-specific rRNA probes. Deep Sea Res., Part II **103:** 185-198. doi:10.1016/j.dsr2.2013.05.034

Brosnahan, M. L. and others 2015. Rapid growth and concerted sexual transitions by a bloom of the harmful dinoflagellate *Alexandrium fundyense* (Dinophyceae). Limnol. Oceanogr. **60:** 2059-2078. doi:10.1002/lno.10155

Brussaard, C. P. 2004. Viral control of phytoplankton populations - a Review. J. Eukaryotic Microbiol. **51:** 125-138. doi:10.1111/j.1550-7408.2004.tb00537.x

Cachon, J. 1964. Contribution à l'étude des péridiniens parasites. Cytologie, cycles évolutifs. Ann. Sci. Nat. Zool **6:** 1-158.

Calbet, A., and M. R. Landry. 2004. Phytoplankton growth, microzooplankton grazing, and carbon cycling in marine systems. Limnol. Oceanogr. **49:** 51-57. doi:10.4319/lo.2004.49.1.0051

Chambouvet, A., P. Morin, D. Marie, and L. Guillou. 2008. Control of toxic marine dinoflagellate blooms by serial parasitic killers. Science **322:** 1254-1257. doi:10.1126/science.1164387

Choi, C. J., and J. A. Berges. 2013. New types of metacaspases in phytoplankton reveal diverse origins of cell death proteases. Cell Death Dis. **4:** e490. doi:10.1038/cddis.2013.21

Cloern, J. E. 1996. Phytoplankton bloom dynamics in coastal ecosystems: A review with some general lessons from sustained investigation of San Francisco Bay, California. Rev. Geophys. **34:** 127-168. doi:10.1029/96rg00986

Crespo, B. G., B. A. Keafer, D. K. Ralston, H. Lind, D. Farber, and D. M. Anderson. 2011. Dynamics of *Alexandrium fundyense* blooms and shellfish toxicity in the Nauset Marsh System of Cape Cod (Massachusetts, USA). Harmful Algae **12:** 26-38. doi:10.1016/j.hal.2011.08.009

Crippen, R., and J. Perrier. 1974. The use of neutral red and evans blue for live-dead determinations of marine plankton (with comments on the use of rotenone for inhibition of grazing). Biotech. Histochem. **49:** 97-104. doi:10.3109/10520297409116949

Erdner, D. L. and others 2008. Centers for oceans and human health: a unified approach to the challenge of harmful algal blooms. Environ. Health **7** (Suppl. 2): S2. doi:10.1186/1476-069x-7-s2-s2

Figueroa, R. I., C. Dapena, I. Bravo, and A. Cuadrado. 2015. The hidden sexuality of *Alexandrium minutum*: An example of overlooked sex in dinoflagellates. Plos One **10:** e0142667. doi:10.1371/journal.pone.0142667

Franklin, D. J., C. P. D. Brussaard, and J. A. Berges. 2006. What is the role and nature of programmed cell death in phytoplankton ecology? Eur. J. Phycol. **41:** 1-14. doi:10.1080/09670260500505433

Garces, E., M. Montresor, J. Lewis, K. Rengefors, D. M. Anderson, and H. Barth. 2010. Phytoplankton life cycles and their impacts on the ecology of harmful algal blooms. Deep Sea Res., Part II **57:** 159-161. doi:10.1016/j.dsr2.2010.01.002

Hallegraeff, G. M. 1993. A review of harmful algal blooms and their apparent global increase. Phycologia **32:** 79-99. doi:10.2216/i0031-8884-32-2-79.1

Jauzein, C., and D. L. Erdner. 2013. Stress-related responses in *Alexandrium tamarense* cells exposed to environmental changes. J. Eukaryotic Microbiol. **60:** 526-538. doi:10.1111/jeu.12065

John, U., R. W. Litaker, M. Montresor, S. Murray, M. L. Brosnahan, and D. M. Anderson. 2014. Formal revision of the *Alexandrium tamarense* species complex (Dinophyceae) taxonomy: The introduction of five species with emphasis on molecular-based (rDNA) classification. Protist **165:** 779-804. doi:10.1016/j.protis.2014.10.001

Kamykowski, D., R. E. Reed, and G. J. Kirkpatrick. 1992. Comparison of sinking velocity, swimming velocity, rotation and path characteristics among six marine dinoflagellate species. Mar. Biol. **113:** 319-328. doi:10.1007/BF00347287

Lilly, E. L., K. M. Halanych, and D. M. Anderson. 2007. Species boundaries and global biogeography of the *Alexandrium tamarense* complex (Dinophyceae). J. Phycol. **43:** 1329-1338. doi:10.1111/j.1529-8817.2007.00420.x

Lu, Y., S. Wohlrab, G. Glöckner, L. Guillou, and U. John. 2014. Genomic insights into processes driving the infection of *Alexandrium tamarense* by the parasitoid *Amoebophrya sp*. Eukaryotic Cell **13:** 1439-1449. doi:10.1128/ec.00139-14

McGillicuddy, D. J. and others 2014. A red tide of *Alexandrium fundyense* in the Gulf of Maine. Deep Sea Res., Part II **103:** 174-184. doi:10.1016/j.dsr2.2013.05.011

Papadopulos, F. and others 2007. Common tasks in microscopic and ultrastructural image analysis using ImageJ. Ultrastruct. Pathol. **31:** 401-407. doi: 10.1080/01913120701719189

Paerl, H. W. 1997. Coastal eutrophication and harmful algal blooms: Importance of atmospheric deposition and groundwater as "new" nitrogen and other nutrient sources. Limnol. Oceanogr. **42:** 1154-1165. doi:10.4319/lo.1997.42.5_part_2.1154

Petitpas, C. M., J. T. Turner, B. A. Keafer, D. J. McGillicuddy, and D. M. Anderson. 2015. Zooplankton community grazing impact on a toxic bloom of *Alexandrium fundyense* in the Nauset Marsh System, Cape Cod, Massachusetts, USA. Harmful Algae **47:** 42-55. doi:10.1016/j.hal.2015.05.010

Ralston, D. K., B. A. Keafer, M. L. Brosnahan, and D. M. Anderson. 2014. Temperature dependence of an estuarine harmful algal bloom: Resolving interannual variability in bloom dynamics using a degree-day approach. Limnol. Oceanogr. **59:** 1112-1126. doi:10.4319/lo.2014.59.4.1112

Segovia, M. A., L. Haramaty, J. A. Berges, and P. G. Falkowski. 2003. Cell death in the unicellular chlorophyte *Dunaliella tertiolecta*. A hypothesis on the evolution of

apoptosis in higher plants and metazoans. Plant Physiol. **132:** 99-105. doi:10.1104/pp.102.017129

Smayda, T. J. 1997. Harmful algal blooms: Their ecophysiology and general relevance to phytoplankton blooms in the sea. Limnol. Oceanogr. **42:** 1137-1153. doi:10.4319/lo.1997.42.5_part_2.1137

Therriault, J., J. Painchaud, and M. Levasseur. 1985. Factors controlling the occurrence of *Protogonyaulax tamarensis* and shellfish toxicity in the St. Lawrence Estuary: freshwater runoff and the stability of the water column. p. 141-146. Anderson DM, White AM, and Baden DG [eds.], Toxic Dinoflagellates. New York: Elsevier.

Turner, J. T., and D. M. Anderson. 1983. Zooplankton grazing during dinoflagellate blooms in a Cape Cod embayment, with observations of predation upon tintinnids by copepods. Mar. Ecol. **4:** 359-374. doi:10.1111/j.1439-0485.1983.tb00119.x

Vardi, A., I. Berman-Frank, T. Rozenberg, O. Hadas, A. Kaplan, and A. Levine. 1999. Programmed cell death of the dinoflagellate *Peridinium gatunense* is mediated by CO_2 limitation and oxidative stress. Curr. Biol. **9:** 1061-1064. doi:10.1016/s0960-9822(99)80459-x

Vardi, A. and others 2012. Host-virus dynamics and subcellular controls of cell fate in a natural coccolithophore population. Proc. Natl. Acad. Sci. USA **109:** 19327-19332. doi:10.1073/pnas.1208895109

Vardi, A. and others 2009. Viral glycosphingolipids induce lytic infection and cell death in marine phytoplankton. Science **326:** 861-865. doi:10.1126/science.1177322

Velo-Suarez, L., M. L. Brosnahan, D. M. Anderson, and D. J. McGillicuddy. 2013. A quantitative assessment of the role of the parasite *amoebophrya* in the termination of *Alexandrium fundyense* blooms within a small coastal embayment. Plos One **8:** e81150. doi:10.1371/journal.pone.0081150

Weise, A. M. and others 2002. The link between precipitation, river runoff, and blooms of the toxic dinoflagellate *Alexandrium tamarense* in the St. Lawrence. Can. J. Fish. Aquat. Sci. **59:** 464-473. doi:10.1139/f02-024

Acknowledgements

The authors are grateful to all members of the Anderson Laboratory at WHOI for their assistance for the collection and analysis of samples, especially to D. Kulis and M. McKenna. This article is a result of research funded by the National Oceanic and Atmospheric Administration Center for Sponsored Coastal Ocean Research ECOHAB program under award no. NA09NOS4780166 to the University of Texas Marine Science Institute (D.L.E) and the Woods Hole Center for Oceans and Human Health by National Science Foundation (NSF) award no. OCE-1314642 and National Institute of Environmental Health Sciences (NIEHS) award no. 1-P01-ES021923-014 to D.M.A. and M.L B. This is publication #ECOHAB839.

Figure Legends

Fig. 1. Map of Western Gulf of Maine showing the location of the study sites within the Nauset Marsh System (NMS; inset). The locations of the two stations sampled for this study are denoted by star symbols.

Fig. 2. Temporal (date) and spatial (depth) dynamics of the *A. fundyense* population at Mill Pond (a) and Salt Pond (b) during 2013 bloom season, from March to May 2013. The maximum mean concentration and the standard deviation of *A. fundyense* cells for each sampling date shows cell abundance as logarithmic scale. In some cases, error bars do not exceed the symbol width.

Fig. 3. Cell mortality in the *A. fundyense* population shown as percentage (mean ± standard deviation) dead cells (left axis, black circles), ROS generation (left axis, white circles) and caspase activity (left axis, grey circles) for associated cell death features in Mill Pond (a) and Salt Pond (b). *A. fundyense* infection rates with *Amoebophrya* spp. maturation stage (left axis, white circles for early stage, grey circles for intermediate stage and black circles for mature stage) and *Amoebophrya* spp. dinospore dynamics (right axis, black dotted line) in Salt Pond are shown in (c). Depth distribution of two loss factors, cell death and infections with *Amoebophrya* spp., in the *A. fundyense* population is shown as proportions of dead cells (mean ± standard error, left axis, white circles 1m, grey circles 3m and black circles 5m) and infected cells (left axis, open diamonds 1m, open triangles 3m and open squares 5m) from 1 m, 3 m and 5 m depths in Salt Pond (d). *A. fundyense* cell densities as presented in Fig. 2 are shown here as interpolated lines (right axis, black solid line) to visualize the impacts of loss factors over the bloom progression.

Fig. 4. Total cell abundance (right axis, line) and the mean cell size (mean ± standard error, left axis, open circles) of *A. fundyense* population over the bloom period in Salt Pond, describing decreases in cell sizes until the peak of the bloom followed by increases as the bloom declines (a). Estimated proportion of *A. fundyense* population as gametes (black), vegetative cells (white) and planozygotes (grey) over the bloom progression in Salt Pond based on the cell size analysis in this study (b).

Fig. 1.

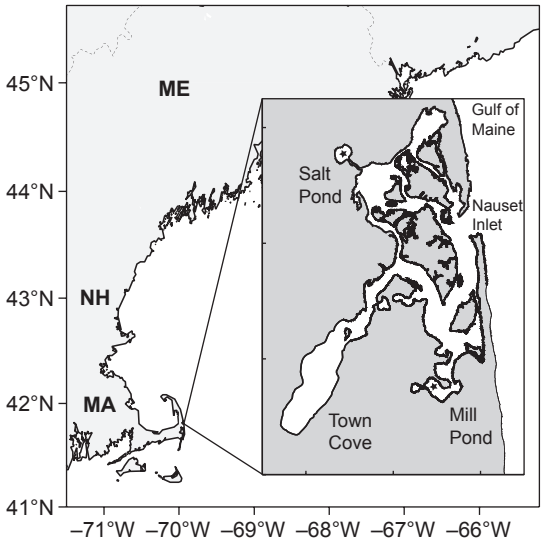

Fig. 2.

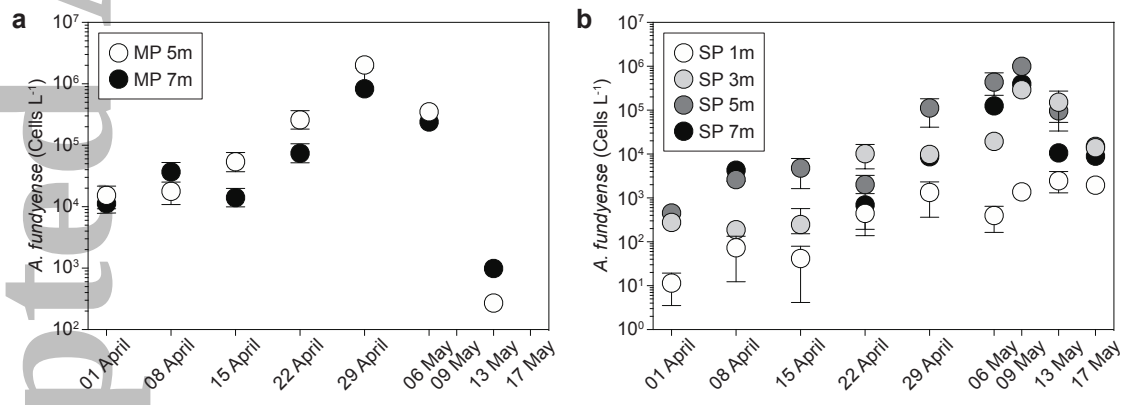

Fig. 3.

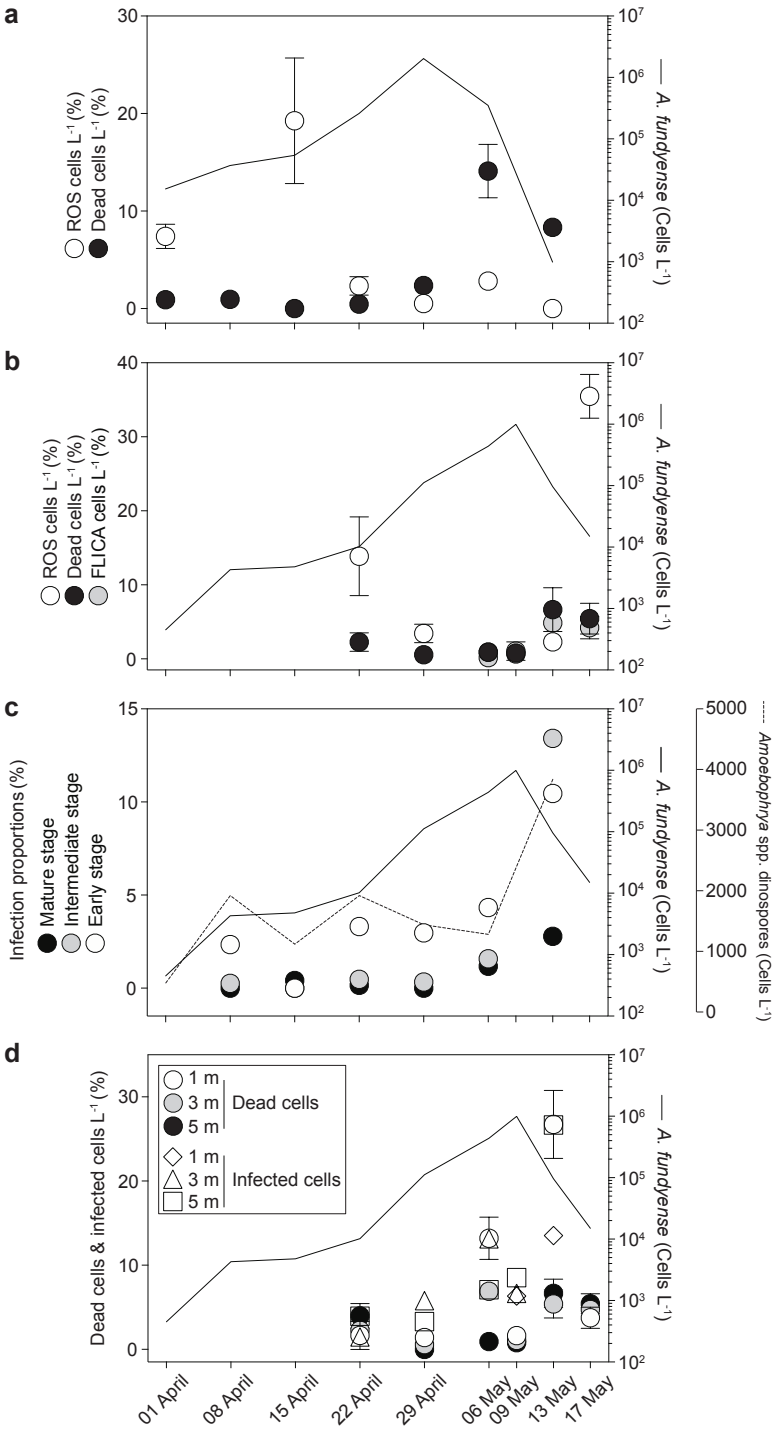

Fig. 4.

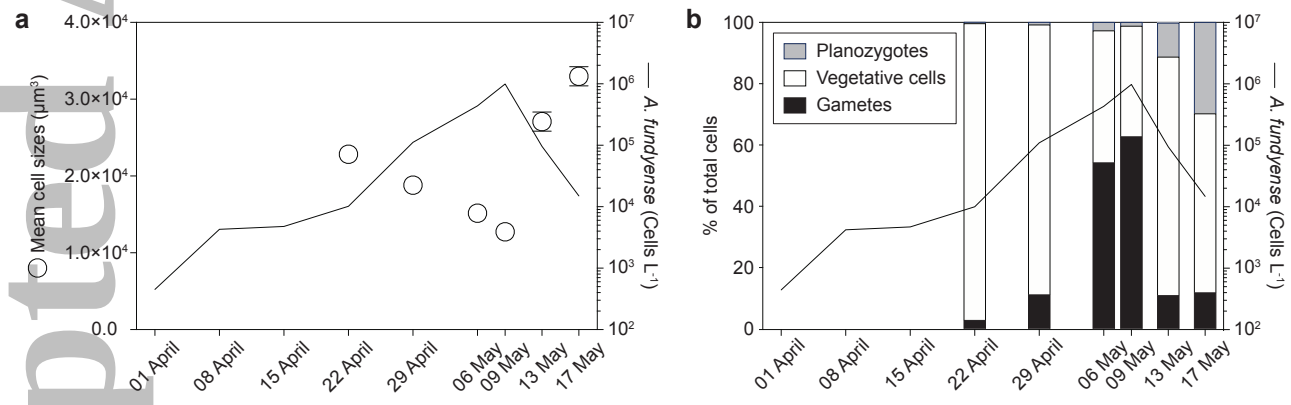

Supplemental Information

Insights into the loss factors of phytoplankton blooms: The role of cell mortality in the decline of two inshore *Alexandrium* blooms

Chang Jae Choi[1,3], Michael L. Brosnahan[2], Taylor R Sehein[2], Donald M. Anderson[2] and Deana L. Erdner[*,1]

[*]Corresponding author: Deana L. Erdner, The University of Texas at Austin, Marine Science Institute, Port Aransas, TX 78373 USA phone: +1 361 749 6719; fax: +1 361 749 6777; e-mail: derdner@utexas.edu

[1]The University of Texas at Austin, Marine Science Institute, Port Aransas, TX 78373 USA

[2]Biology Department, Woods Hole Oceanographic Institution, Woods Hole, MA 02543 USA

[3]Current address: Monterey Bay Aquarium Research Institute, 7700 Sandholdt Road, Moss Landing, CA 95039 USA

Content of this file:

Tables S1, S2

Figure S1

Table S1. Descriptive statistics on *A. fundyense* cell size (μm^3) distributions over the bloom period at Salt Pond. The significance of differences among all samples was analyzed by means of the Kolmogorov-Smirnov test.

	22 April	29 April	6 May	9 May	13 May	17 May
Number of cells examined	250	361	754	773	311	389
Minimum	11073.1	8317.71	3625.68	2649.15	6145.84	5708.47
25% Percentile	18700.6	15028.1	10046.7	6873.46	19320.2	20397.9
Median	22193.1	17631.3	12975.4	10652.8	27400.1	29597.1
75% Percentile	26626.8	21226.9	17498.1	16575.8	33206.1	42684.2
Maximum	67964.5	82973.7	87104.0	66517.4	67375.5	95345.3
Mean	22848.7	18824.3	15172.3	12744.1	27091.9	32987.4
S.D	5904.06	6350.19	8752.83	8030.2	10677.3	17477.3
S.E.M	373.405	334.221	318.759	288.826	605.452	886.135
P value	<0.0001	<0.0001	<0.0001	<0.0001	<0.0001	<0.0001

Table S2. Estimated daily contribution of cell loss processes to bloom decline from all depths.

	Cell abundance	% Infection (day^{-1})	Cell loss to infection (day^{-1})	% Daily loss contribution by infection	% Cumulative loss contribution by infection	% Cell death (day^{-1})	Cell loss to death (day^{-1})	% Daily loss contribution by cell death	% Cumulative loss contribution by cell death
9 May	422922[1]	2.79[1]	11783	7.05	7.05	2.10[1]	8861	5.30	5.30
10 May	255696[2]	5.09[2]	13025	13.63	9.44	8.73[2]	22313	23.35	11.86
11 May	160131[2]	7.40[2]	11852	19.80	11.36	15.36[2]	24593	41.09	17.28
12 May	100282[2]	9.71[2]	9737	23.35	12.73	21.99[2]	22051	52.88	21.36
13 May	58579[1]	12.02[1]	7039	36.57	13.93	28.62[1]	16766	87.10	24.66
14 May	39330[2]	12.98[2]	5106	34.74	14.70	24.07[2]	9466	64.40	26.12
15 May	24631[2]	13.95[2]	3436	37.32	15.21	19.51[2]	4807	52.21	26.71
16 May	15425[2]	14.92[2]	2301	42.53	15.57	14.96[2]	2308	42.66	26.92
17 May	10015[1]	15.88[2]	1591	40.12	15.80	10.41[1]	1043	26.29	26.92

[1] Observed value; [2] Calculated value

Fig. S1. Changes of the *A. fundyense* cell size distributions over the bloom period in Salt Pond. The mean size of the cells during the early phase of the bloom (22 April) is denoted by the vertical black lines as a baseline of the cell size. The mean cell size at each sampling time is indicated by red lines. The overall shift in the mean cell sizes is represented by the arrows.

Fig. S1.